

Hydrogen peroxide treatment induced rectifying behavior of Au/*n*-ZnO contact

Q. L. Gu, C. C. Ling,^{a)} X. D. Chen, C. K. Cheng, A. M. C. Ng, C. D. Beling, S. Fung, A. B. Djurišić, and L. W. Lu
Department of Physics, The University of Hong Kong, Pokfulam Road, Hong Kong, People's Republic of China

G. Brauer
Institut für Ionenstrahlphysik und Materialforschung, Forschungszentrum Dresden-Rossendorf, Postfach 510119, D-01314 Dresden, Germany

H. C. Ong
Department of Physics, Chinese University of Hong Kong, Shatin, Hong Kong, People's Republic of China

(Received 26 January 2007; accepted 13 February 2007; published online 19 March 2007)

Conversion of the Au/*n*-ZnO contact from Ohmic to rectifying with H₂O₂ pretreatment was studied systematically using *I*-*V* measurements, x-ray photoemission spectroscopy, positron annihilation spectroscopy, and deep level transient spectroscopy. H₂O₂ treatment did not affect the carbon surface contamination or the *E*_C-0.31 eV deep level, but it resulted in a significant decrease of the surface OH contamination and the formation of vacancy-type defects (Zn vacancy or vacancy cluster) close to the surface. The formation of a rectifying contact can be attributed to the reduced conductivity of the surface region due to the removal of OH and the formation of vacancy-type defects. © 2007 American Institute of Physics. [DOI: 10.1063/1.2715025]

Zinc oxide is a wide band gap semiconductor which has recently attracted extensive attention because of its potential for a wide variety of applications, such as optoelectronic, high frequency, gas sensing, piezoelectric and transparent devices, etc.¹ Fabricating high quality metal contact to ZnO is an important step for successful device fabrication because a metal-semiconductor structure is one of the essential structures for many devices. However, reports of successful rectifying metal/*n*-ZnO contact have been scarce. The metals used include Au,²⁻⁹ Ag,^{6,10} Pt,¹¹⁻¹³ and Pd.^{2,3,14,15} It has also been shown that surface treatments such as H₂O₂,¹² sulfide,¹³ ozone,¹¹ and plasma^{4,9} can improve the rectifying contact quality (increase the barrier height, decrease the reverse bias leakage current, and achieve an ideality factor approaching unity). While several explanations, such as good surface morphology, removal of C and OH contamination, and reduction in surface conductivity, have been proposed, the mechanisms behind contact quality improvements are still controversial and not well understood.

We have systematically studied the influence of the H₂O₂ pretreatment duration and temperature on the properties of Au/*n*-ZnO contacts. As the observed phenomenon may involve more than one physical process, x-ray photoemission spectroscopy (XPS), scanning electron microscopy (SEM), positron annihilation spectroscopy (PAS), and deep level transient spectroscopy (DLTS) were used to investigate the influence of contamination, morphology, and defects on the electrical properties of the fabricated Au/ZnO contacts. The ZnO sample used was melt-grown undoped *n*-type ZnO obtained from the Cermet Inc., U.S. The carrier concentration of the as-received material was found to be $5 \times 10^{16} \text{ cm}^{-3}$. Au contacts having a diameter of 0.5 mm and a thickness of 50 nm were fabricated by thermal evaporation

under a vacuum of 10⁻⁶ Torr. The time and temperature of the H₂O₂ pretreatment were systematically varied in the ranges of 1–30 min and from room temperature to the boiling temperature of H₂O₂, respectively.

The *I*-*V* data of the Au/*n*-ZnO contacts without H₂O₂ pretreatment shown in Fig. 1 clearly showed the nonrectifying property of the contact. On the other hand, all the samples with H₂O₂ pretreatment became rectifying, but the ideality factor *n*, the Schottky barrier height ϕ_S , and the leakage current *I*_{leak} were dependent on the pretreatment temperature and time, having values in the ranges of *n* = 1.15–2.89, ϕ_S = 0.35–0.65 eV, and *I*_{leak} = 10⁻⁹–10⁻⁴ A (as the reverse bias *V*_R = -1 V). The best performing diode (*I*-*V* curve shown in Fig. 1) was obtained by preetching the sample in H₂O₂ at 100 °C for 3 min. Its ideality factor, Schottky barrier height, and leakage current at -1 V were

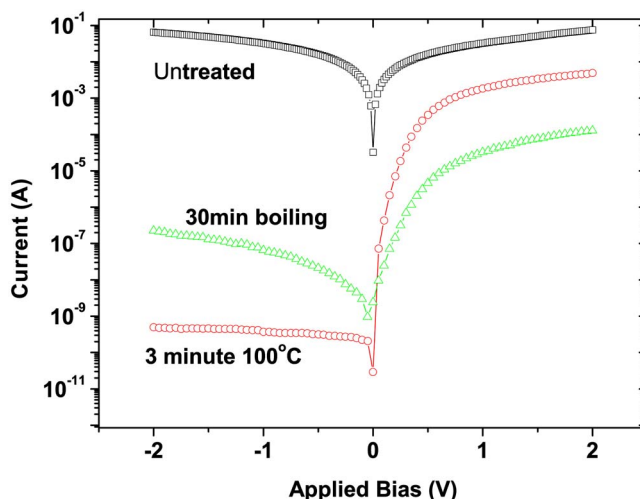


FIG. 1. (Color online) *I*-*V* data of the Au/*n*-ZnO samples with different H₂O₂ pretreatments.

^{a)} Author to whom correspondence should be addressed; electronic mail: ccling@hku.hk

TABLE I. Intensities of XPS signals (in atomic ratio) found in the nontreated and the 3 min 100 °C H₂O₂ treated *n*-type ZnO samples.

	C (%)	O (%)	OH (%)	Zn (%)	Zn:O ratio on surface
Nontreated	14.2	20.9	26.1	38.8	1.86
100 °C, 3 min	14.2	55.2	1.3	22	0.40

found to be 1.15, 0.63 eV and 4.2×10^{-9} A, respectively. The SEM images (not included) showed that the as-grown ZnO sample had a smooth surface, and the 3 min 100 °C H₂O₂ treatment increased the surface roughness and induced appearance of submicron grains on the surface. The worst performing diode was the one pretreated with the longest time period (i.e., 30 min) and the highest temperature (i.e., boiling H₂O₂), which had $n=2.89$, $\phi_S=0.53$ eV, and leakage current equal to 7.8×10^{-8} A (at -1 V). The SEM image showed that the surface was damaged after the 30 min boiling H₂O₂ treatment.

XPS data revealed that all the samples contained carbon impurities. The C 1s (285.36 keV) signal, which disappeared after Ar sputtering, corresponded to a thickness of about 50 Å implying that the detected C impurity resided at the sample surface. As shown in Table I, the carbon concentration could not be removed with the H₂O₂ treatments. The surface carbon contamination therefore does not seem to have any significant adverse influence on the formation of Au Schottky contact. The O 1s signal was well fitted by a two-peak fit having binding energies of 531.25 and 532.76 eV, which corresponded to oxygen bound to the lattice and oxygen in the OH impurity.⁴ 3 min H₂O₂ treatment results in a significant reduction of the OH intensity from 26.1% to 1.3%, as well as the loss of Zn and the reduction of the Zn:O ratio from 1.85 to 0.40. OH leads to the formation of a high conductivity accumulation layer on both the polar faces of ZnO.⁴ The correlation between the OH removal and the improvement of the metal-ZnO Schottky contacts has also been observed by Coppa *et al.*⁴ and Mosbacher *et al.*⁹

PAS was employed to study the vacancy-type defects close to the surface.^{16,17} Monoenergetic positrons were implanted into the sample with variable positron energy (up to ~30 keV), hence varying the positron implantation depth. The implanted positrons will then be thermalized, undergo diffusion, possibly be trapped by vacancy-type defects, and finally annihilate with an electron emitting two gamma photons with energies of ~511 keV, providing information about the electronic environment at which the positron annihilates. The Doppler broadening of the annihilation radiation was parametrized by the *S* parameter, defined as the ratio of the central region count (i.e., A_C in Fig. 2) to the total count and is thus associated with the fraction of positrons annihilating with the valance electrons. The *W* parameter (wing parameter) is defined as the ratio of a fixed pair of high energy windows (i.e., A_{W1} and A_{W2} in Fig. 2) to the total counts, and is thus related to fraction annihilating core electrons. As a positron trapped in the vacancy state has less probability to annihilate with the core electrons having higher momentum relative to the valance electrons, annihilation events originated from the vacancy state would be less Doppler broadened and would thus contribute a larger *S* parameter (smaller *W* parameter) as compared to the bulk state.

The *S* parameter as a function of the positron implanting energy of three ZnO is shown in Fig. 2. The *S*(*E*) data were fitted by the source code VEPFIT,¹⁸ where the dynamics of the implanted positrons were described by the diffusion-trapping-annihilation equation considering positron implantation, positron diffusion, positron trapping into vacancy, and subsequent annihilation at different states. The resultant *S* parameter measured at different implanting energy is given by $S(E) = \sum f_i S_i$, where f_i and S_i are the fraction and the characteristic *S* parameter of positron annihilating at site *i*. For the untreated sample, a single layer model was found to give a good fitting to the data. The positron diffusion length L_{eff} was found to be 72 ± 2 nm. The *S*(*E*) data of the 3 min 100 °C and the 30 min boiling treated samples in Fig. 2 clearly show shoulders implying the existence of at least one defective layer corresponding to the high value of the *S* parameter. Finally, the SE curves of these two samples were well fitted by the three layer model with the results shown in Table II. The characteristic bulk *S* parameters and the effective positron diffusion length of the three samples were found to be $S_b=0.5096$ nm and $L_B=72$ nm. The first and the second layers of the two H₂O₂ treated samples had values of *S* parameters higher than the bulk and L_+ smaller than the bulk indicative of the creation of vacancy-type defects in these two layers by the H₂O₂ treatment. Moreover, the fact that $S_1 > S_2$ and $L_1 < L_2$ implied that the first layer was more defective than the second layer. The defective region extended to widths of 393 and 422 nm for the 3 min 100 °C treated and the 30 min boiling treated samples, respectively. The SW plot of the data accumulated from the 3 min 100 °C, 30 min 100 °C, and 30 min boiling H₂O₂ treated samples is shown in Fig. 3, which clearly shows a straight line. This

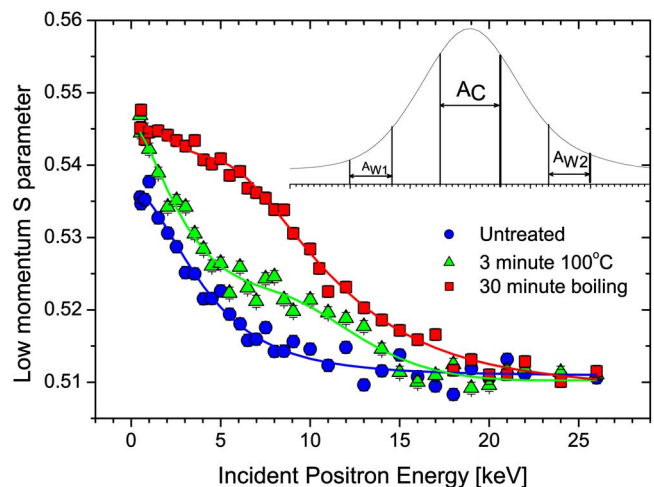


FIG. 2. (Color online) *S*(*E*) data of the untreated (circle), the 3 min 100 °C H₂O₂ treated (triangle), and the 30 min boiling H₂O₂ treated *n*-ZnO samples. The inset illustrates the definition of the *S* parameter and the *W* parameter. The solid lines are the fitted curves.

TABLE II. Fitted results of the $S(E)$ data shown in Fig. 2. The indices S , 1, 2, and B in the S parameter and the diffusion length L denote the surface, the first layer, the second layer and the bulk, respectively, while X_1 and X_2 are the boundary positions of the first and the second layers, respectively.

	Surface	First layer	Second layer	Bulk
Untreated	$S_S=0.5373$	NA	NA	$S_B=0.5109$ $L_B=72$ nm
3 min 100 °C	$S_S=0.5453$	$S_1=0.5224$ $L_1=35$ nm $X_1=56$ nm	$S_2=0.5212$ $L_2=48$ nm $X_2=393$ nm	$S_B=0.5092$ $L_B=70$ nm
30 min 185 °C	$S_S=0.5465$	$S_1=0.5401$ $L_1=29$ nm $X_1=223$ nm	$S_2=0.5202$ $L_2=37$ nm $X_2=422$ nm	$S_B=0.5086$ $L_B=72$ nm

implies that the vacancies created in the H_2O_2 treatment irrespective of time and temperature were of the identical type.¹⁶ Since O vacancy has low binding energy and thus does not trap positrons at room temperature,^{19–23} the vacancy defects created by H_2O_2 treatment are Zn-vacancy-related defects and vacancy clusters, although the Doppler technique used in the present study cannot offer an unambiguous distinction between the two possibilities. XPS data (in Table I) showed that after the H_2O_2 treatment, the Zn:O ratio significantly reduced to a Zn insufficient value of 0.40. It is thus speculated that the vacancy-type defects formed are Zn vacancy or Zn-vacancy cluster. As Zn vacancy is known to be an acceptor, the H_2O_2 etching would thus possibly have the effect of forming a defective layer having a relatively low conductivity.

In the DLTS measurements, a deep level having the activation energy of $E_a=0.31$ eV was identified in all of the diodes tested. This defect was also found in some other n -type ZnO structure not pretreated by H_2O_2 .^{24,25} The deep level concentrations found in the 3 min 100 °C, the 30 min 100 °C, the 3 min 185 °C, and the 30 min 185 °C H_2O_2 pretreated samples were observed to be independent of the reverse bias applied during the DLTS measurement, the treatment temperature, or the treatment duration (with values of 8.8×10^{14} , 1.0×10^{15} , 1.2×10^{15} , and 8.6×10^{14} cm⁻³, respectively). This implies that the deep level is (1) a uni-

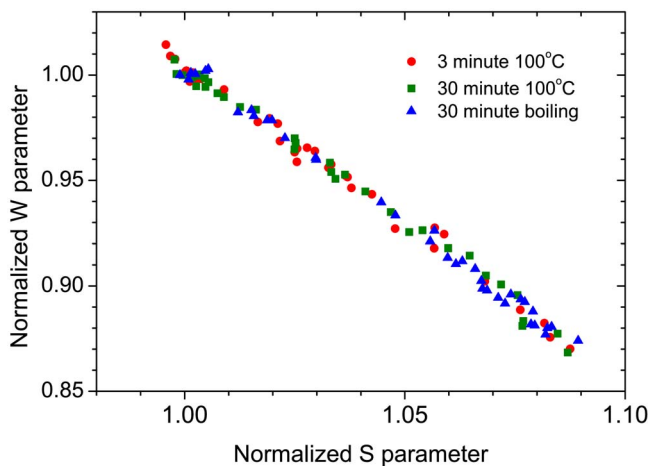


FIG. 3. (Color online) $S(E)$ plot of the data obtained from the 3 min 100 °C, the 30 min 100 °C, and the 30 min boiling H_2O_2 treated n -ZnO samples.

formly distributed bulk defect, (2) not associated with the vacancy-type defect as detected by PAS, and (3) thus not related to the H_2O_2 treatment.

In conclusion, Ohmic to rectifying conversion was observed on the Au/ n -ZnO contact with the pretreatment of H_2O_2 . A good quality Schottky contact was obtained with $n=1.15$, $\phi_S=0.63$ eV, and $I_{leak}(V_R=-1$ V) $=4.2 \times 10^{-9}$ A. The good performance of a Au Schottky contact was associated with the removal of OH surface contamination and creation of a defective surface region, containing zinc vacancy or vacancy cluster. Both of these effects result in the overall reduction of the conductivity of the surface layer. A deep level with $E_A=0.31$ eV was observed in all the samples but was suggested to be unrelated to the H_2O_2 treatment.

This project was supported by the CERG, RGC, HKSAR (Nos 7032/04 and 7036/07), and the University Development Fund Grant, The University of Hong Kong.

¹Ü. Özgür, Yu. I. Alivov, C. Liu, A. Teke, M. A. Reshchikov, S. Doğan, V. Avrutin, S.-J. Cho, and H. Morkoç, *J. Appl. Phys.* **98**, 041301 (2005).

²C. A. Mead, *Phys. Rev. Lett.* **14**, 219 (1965).

³C. Neville and C. A. Mead, *J. Appl. Phys.* **41**, 3795 (1970).

⁴B. J. Coppa, R. F. Davis, and R. J. Nemanich, *Appl. Phys. Lett.* **82**, 400 (2003).

⁵F. D. Auret, S. A. Goodman, M. Hayes, M. J. Legodi, H. A. van Laarhoven, and D. C. Look, *Appl. Phys. Lett.* **79**, 3074 (2001).

⁶A. Y. Polyakov, N. B. Smirnov, E. A. Kozhukhova, V. I. Vdovin, K. Ip, Y. W. Heo, D. P. Norton, and S. J. Pearton, *Appl. Phys. Lett.* **83**, 1575 (2003).

⁷G. Yuan, Z. Ye, L. Zhu, J. Huang, Q. Qian, and B. Zhao, *J. Cryst. Growth* **268**, 169 (2004).

⁸D. C. Oh, J. J. Kim, H. Makino, T. Hanada, M. W. Cho, T. Yao, and H. J. Ko, *Appl. Phys. Lett.* **86**, 042110 (2005).

⁹H. L. Mosbacher, Y. M. Strzhemechny, B. D. White, P. E. Smith, D. C. Look, D. C. Reynolds, C. W. Litton, and L. J. Brillson, *Appl. Phys. Lett.* **87**, 012102 (2005).

¹⁰H. Sheng, S. Muthukumar, N. W. Emanetoglu, and Y. Lu, *Appl. Phys. Lett.* **80**, 2132 (2002).

¹¹K. Ip, B. P. Gila, A. H. Onstine, E. S. Lambers, Y. W. Heo, K. H. Baik, D. P. Norton, S. J. Pearton, S. Kim, J. R. LaRoche, and F. Ren, *Appl. Phys. Lett.* **84**, 5133 (2004).

¹²S. H. Kim, H. K. Kim, and T. Y. Seong, *Appl. Phys. Lett.* **86**, 112101 (2005).

¹³S. H. Kim, H. K. Kim, and T. Y. Seong, *Appl. Phys. Lett.* **86**, 022101 (2005).

¹⁴H. von Wenckstern, E. M. Kaidashev, M. Lorenz, H. Hochmuth, G. Biehne, J. Lenzner, V. Gottschalch, R. Pickelhain, and M. Grundmann, *Appl. Phys. Lett.* **84**, 79 (2004).

¹⁵C. Weichsel, O. Pagni, and A. W. R. Leitch, *Semicond. Sci. Technol.* **20**, 840 (2005).

¹⁶*Positron Beams and their Applications*, edited by P. Coleman (World Scientific, Singapore, 2000).

¹⁷P. J. Schultz and K. G. Lynn, *Rev. Mod. Phys.* **60**, 701 (1988).

¹⁸A. van Veen, H. Schut, J. de Vries, R. A. Hakvoot, and M. R. Ijpma, *AIP Conf. Proc.* **218**, 171 (1990).

¹⁹G. Brauer, W. Anwand, W. Skorupa, J. Kuriplach, O. Melikhova, and C. Moisson, *Phys. Rev. B* **74**, 045208 (2006).

²⁰F. Tuomisto, V. Ranki, K. Saarinen, and D. C. Look, *Phys. Rev. Lett.* **91**, 205502 (2003).

²¹T. Koida, S. F. Chichibu, A. Uedono, A. Tsukazaki, M. Kawasaki, T. Sota, Y. Segawa, and H. Koinuma, *Appl. Phys. Lett.* **82**, 532 (2003).

²²S. Brunner, W. Puff, A. G. Balogh, and P. Mascher, *Mater. Sci. Forum* **363–365**, 141 (2001).

²³Z. Q. Chen, M. Maekawa, S. Yamamoto, A. Kawasuso, X. L. Yuan, T. Sekiguchi, R. Suzuki, and T. Ohdaira, *Phys. Rev. B* **69**, 035210 (2004).

²⁴H. von Wenckstern, R. Pickelhain, H. Schmidt, M. Brandt, G. Biehne, M. Lorenz, M. Grundmann, and G. Brauer, *Appl. Phys. Lett.* **89**, 092122 (2006).

²⁵J. C. Simpson and J. F. Cordaro, *J. Appl. Phys.* **63**, 1781 (1988).